DESERT 2021, 26(2): 187-203
DOI: 10.22059/jdesert.2021.309637.1006791

RESEARCH PAPER

# Monitoring Dynamic Distribution of Surface Soil Moisture Using SMAP data in Simineh-Zarrineh Catchment (Semi-arid region), NW of Iran

**Khaled Haji Maleki[1,*], Ali Reza Vaezi[1], Fereydoon Sarmadian[2], Jamal Ahmadaali[3]**

[1] Soil Science Department, Faculty of Agriculture, University of Zanjan, Iran
[2] Soil Science Dept., Faculty of Agriculture, University of Tehran, Iran
[3] Agricultural Engineering Research Institute of Urmia, West Azerbaijan, Iran

Received: 08 September 2020, Revised: 12 May 2021, Accepted: 16 May 2021


**Abstract**
Soil moisture (SM) is believed to be an impressive factor in hydrological process, agricultural productivity, and monitoring dangerous outcomes of climate changes. The present study aimed to monitor and recognize the pattern of spatial and temporal variation of SMAP soil moisture in five subcatchments of Simineh-Zarrineh catchment in northwest of Iran from 2015 to 2017. Precipitation data of 35 meteorological stations and 287 soil moisture points were derived from the SMAP and used to monitor SM variations in the time scale. The results indicated that the SM variations are subject to precipitation variations throughout the monthly scale in the catchment. In all the seasons of this period, SM was found to have a decreasing trend from north to south of the catchment. On the contrary, no such constant pattern was observed from east to west. Oscillation SM patterns in this period were completely coordinated with the precipitation pattern. The determination coefficient between monthly SMAP soil moisture and precipitation for each subcatchment was 0.9, 0.83, 0.7, 0.84, and 0.71 for Bokan, Saqqez, Takab, Saeinqaleh, and Miandoab subcatchments, respectively. Spatial variability of standard deviation for SM values was used to find the amount of deviation from the average value during dry and wet seasons . The results revealed that in the seasonal scale, northwestern (0.067 to 0.069 $cm^3.cm^3$) and eastern parts (0.057 to 0.061 $cm^3.cm^3$) of the study area had higher values of the SM standard deviations in autumn. Additionally, according to the findings, a high value of standard deviation was observed in autumn because of irregular precipitation events and fluctuation of the temperature.

**Keywords:** Precipitation, Urmia Lake, Standard deviation, Temporal variation, Soil water content

## Introduction

Soil moisture is a generously dynamic state variable that affects principle hydrological phenomena, such as evaporation, infiltration, and runoff. It is also important for the control and allocation of water resources, anticipation of drought, agricultural yield, and supervision of ecosystem reaction to climate changes (Babaeian *et al.*, 2016). Information about SM status is a critical factor for irrigation and enhanced agriculture yield (Brocca et al., 2014b). It is notable that remotely sensed data provide particularly effective tools for large-scale monitoring of soil water content near the land surface (0–5 cm). The SM values is significantly correlated with soil optical reflection (Babaeian *et al*., 2016; Zeng *et al.*, 2016), thermal emission (Hassan-Esfahani *et al.,* 2015), and microwave backscatter (Mladenova *et al.*, 2014). The ability to determine the spatial and temporal distribution of soil moisture would be significantly conducive to understanding the earth as an integrated system. The volume of soil moisture is small compared with other components of the hydrologic cycle; nonetheless, it is of

[*] Corresponding author e-mail: Khaled.hajimaleki@znu.ac.ir

fundamental importance to several hydrological, biological, and biogeochemical processes (Legates *et al.*, 2011; Wang *et al.*, 2019).

On account of this issue, the NASA's Soil Moisture Active Passive (SMAP) mission was launched on January 31st, 2015. The objective of the mission is global mapping of high-resolution surface soil moisture and landscape freeze/thaw state (Entekhabi *et al.*, 2010). SMAP utilizes L-band radar and radiometer sharing a rotating 6-meter mesh reflector antenna. The basic premise of the mission was that merging of the high-resolution active (radar) and coarse-resolution, but high-sensitivity passive (radiometer) L-band observations, would enable an unprecedented combination of accuracy, resolution, coverage, and revisit-time for soil moisture and freeze/thaw state retrievals (Entekhabi *et al.*, 2010; Das *et al.*, 2014).

Various modeling methods, hypotheses, and approaches of predicting auxiliary variables are used to recover soil water information from active and passive microwave sensors, which oriented to differences in predicted soil moisture; these differences are over and above those caused by the differences in the electromagnetic frequency and engineering utilized to gather the radiometric data (Owe *et al.*, 2000). Passive microwave sensors, like SMOS[†], SMAP, and Aquarius, evaluate brightness temperature, which is affected by the differences in surface soil moisture. Meanwhile, it also on the basis of certain parameters, for example, surface temperature, vegetation water content, and surface roughness and/or topography. Most radiative transfer models used to predict surface soil moisture from passive microwave sensors are developed across bare to low biomass vegetative surfaces. A good representation of soil moisture conditions could contribute to enhancing the predicting of precipitation, temperature, droughts, and floods (Brocca *et al.*, 2012; Chen *et al.*, 2011; Miralles *et al.*, 2012; Taylor., 2012). For numerous large-scale utilizations, soil moisture maps are essential. As a result, several studies have been conducted to obtain such information.

In numerous works, spatial distribution of SM has been analyzed; for example, Su *et al.* (2016) investigated the spatio-temporal variation of Essential Climate Variable (ECV) soil moisture dataset. Based on their results, it could be effective on the parameters from 1988 to 2013 in Tarim River basin. Moreover, they demonstrated that the (ECV) soil moisture could control the large-scale dynamics of regional water cycle quite sufficiently, perfectly showing concurrence with in situ data in their seasonal and inter annual variability. Statistical analysis has recommended that the soil moisture variability in the Tarim River basin is further affected by precipitation and temperature is less impressive on controlling soil moisture variability. Champagne *et al.* (2016) assessed satellite surface soil moisture from SMOS and Aquarius for application in agricultural landscapes in Canada. Their results indicated that SMOS overestimates soil moisture after precipitation events in comparison with the in situ observation; this was not compatible for each site and each period of time. The SMOS was discovered to underestimate desiccation events in comparison with the in situ observation.

Spatial variability of soil moisture is known to rise with observation scale (Das and Mohanty, 2008), where the variability is connected to the average soil moisture content for a given scale, like an outcome of prevailing surface processes at work. Famiglietti et a*l.* (2008) demonstrated that the soil moisture spatial distribution was affected by landscape attributes on hillslopes whereas Hupet and Vanclooster (2002) concluded that soil spatial structure and topography were unnecessary parameters and LAI [‡] affected variation of soil moisture through evapotranspiration. In the investigation of some soil moisture datasets, Brocca *et al.* (2007) reported that over different scales, in semi-arid regions, variation of soil moisture increased when soil got wetter whereas humid regions tended to have larger variability throughout become dry. The monitoring effect of this connection is the pattern of precipitation. When the

[†] Soil Moisture and Ocean Salinity
[‡] Leaf Area Index

local meteorology outcomes in non-uniform precipitation, the heterogeneous wetting results in enhanced soil moisture variation (Famiglietti *et al.*, 2008; Vivoni *et al.*, 2008); meanwhile, when precipitation is uniform and at smaller scales, precipitation seems to decrease in the variation of soil moisture (Das and Mohanty, 2008; Ryu and Famiglietti, 2006). The predominant phenomena determining soil moisture variability are the result of the alteration from control of infiltration in wet situation to control by drainage and evapotranspiration in dry situation (Peters-Lidard *et al*., 2001). At basin to watershed scales, soil moisture is less likely to be normally distributed since soil moisture distribution is not any more the outcome of accidental phenomena, but rather structured by vegetation, topography, precipitation, and soil properties (Parada and Liang, 2008).

Although in situ soil moisture is not gauged in all areas of Iran, measurement limitation does not provide dynamic spatio-temporal variations for large-scale in a number of functions. However, in this study area, where soil moisture observation there are not available with suitable spatial and temporal density, it is not possible to monitor a precise large-scale and predict soil moisture based on the in situ observation (Al-Yaari *et al.,* 2014a). Therefore, the use of remotely sensed data, which utilize images retrieved from either passive or active microwave sensors, are suggested owing to their accessibility, global coverage, and verified preciseness. Thus, studying dynamic distribution of soil moisture at spatio-temporal scale is of great necessity in the catchments for recognition soil moisture variation patterns in long term. The present research was conducted for the following objectives : (i) analyzing the spatial and temporal variation in soil moisture from 2015 to 2018; (ii) detecting the patterns of soil moisture dynamic distribution in monthly and seasonal scales; (iii) showing the influence of precipitation variability on the sptio-temporal variation of soil moisture.

## Materials and Methods

*Study area*

The Simineh-Zarrineh catchment is located in the northwest region of Iran (35⁰42′14″-37⁰44′31″N, 45⁰31′32″- 47⁰22′21″ E) with an area of 17625 km$^2$. In the catchment irregular topography, the existence of two permanent streams and different land uses were found with elevation variability between 1254 to 3389 meters above the sea level. Climatically, the catchment has cold season with abundant rain from November to April, the remaining months correspond to dry season (IRAN MINISTRY OF ENERGY., 2014).

Figure 1 depicts the situation and general attributes of the catchment, subcatchment, land use, and rivers. This area belongs to a semi-arid hilly region, with an average annual temperature of nearly 10.9 °C and an average annual precipitation of 348 mm. The precipitation happened mostly during the autumn and winter from October to February.

This area is located in the semi-arid region and provides a large proportion of Urmia Lake basin water requirement as a largest catchment with extensive agricultural activities. Simineh-Zarrineh catchment is located in the mountain chain region in the northwest of Iran. The catchment contains five subcatchments, including Bokan, Saqqez, Takab, Saeinqaleh, and Miandoab.

The Zarrinehrud and Siminehrud streams are perennial rivers in this catchment with the greatest discharge of around 3 billion m$^3$/yr. From 1995 to 2014, these rivers were considered as permanent streams in the area with many natural and social potentials. These streams have resulted in the improvement of agricultural actions in this catchment. These streams basins cover around 52% of the total annual flow inlet to the Urmia Lake annually. The length and basin area of Zarrinehrud River and Siminehrud River are about 240, 200 km and 11642 and 5921 km$^2$, respectively (Ahmadaali *et al*., 2018). Dry land is the dominant land use, with cyclic drought influencing many of the areas for the time period studied. The dominant crop in dry lands are barely and wheat and in irrigated agricultural land, they are sugar beet, alfalfa, and garden. In this area, water scarcity intimidated economic improvement, maintainable human occupations, and environmental characteristics (Urmia Lake Restoration National Committee, 2015).

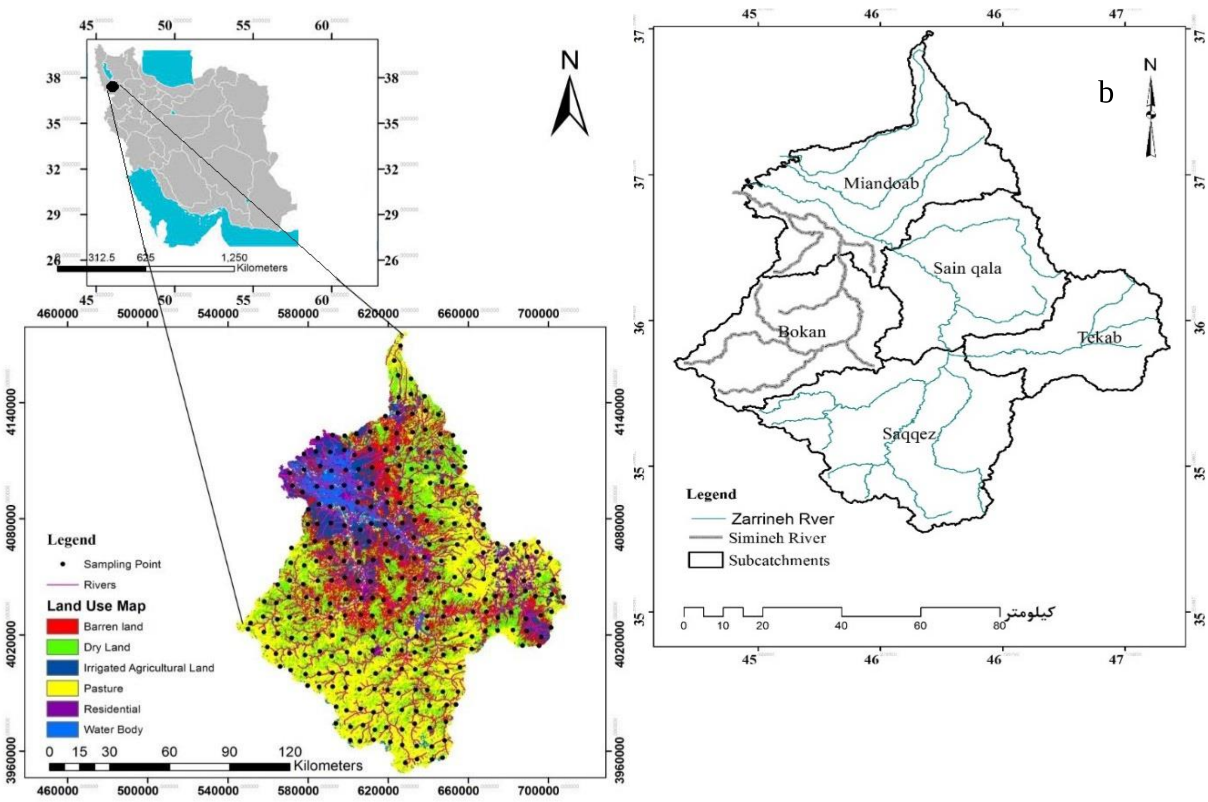


**Figure 1.** Geographical location of the Simineh-Zarrineh catchment (a) and subcatchments (b) in northwest of Iran

*Data collection*

The SMAP satellite was launched on January 2015 by the NASA[§] (Entekhabi *et al*., 2010). It provides SM data that encompass the top 5 cm of the soil surface with a preciseness of 0.04 $cm^3$ and a spatial resolution of 3, 9, and 36 km. It also covers the globe every three days (Das *et al.*, 2011; Reichle *et al.*, 2015). The L-band SMAP satellite has been planned with the outstanding subject of measuring and monitoring SM changes (Entekhabi *et al.,* 2010). According to the SMAP, there are seven advanced SM data as levels 2, 3, and 4, which establish surface and root zone SM. In this study, the level 4 data (L4_SM) was used during 32 months from April 2015 to December 2017 in order to investigate the spatio-temporal variation of SM by 287 observation SMAP points in the catchment. The number of soil moisture observation pixel in all the subcatchments and statistical summaries of soil characteristics in the entire catchment are represented in Tables 1 and 2.

[§] National Aeronautics and Space Administration

**Table 1.** The number of SM observations, the mean precipitation and mean temperature in the subcatchments across the Simineh-Zarrineh catchment (Bokan)

| Subcatchment | Percentage of area | Number of SM observations | Mean annual precipitation (mm) | Mean annual temperature (◦C) |
|---|---|---|---|---|
| Bokan | 17.35 | 51 | 368.5 | 11.8 |
| Saqqez | 26.31 | 75 | 393.1 | 9.6 |
| Takab | 13.05 | 38 | 352.3 | 10.4 |
| Saeinqaleh | 19.27 | 56 | 334.7 | 11.5 |
| Miandoab | 24.02 | 67 | 351.5 | 12.2 |

**Table 2.** Statistical summary of soil characteristics

| Soil parameters | Min. | Max. | Mean | Std. deviation | Coefficient of variation | Skew | Kurtosis | Kolmogorov-Smirnov statistic |
|---|---|---|---|---|---|---|---|---|
| Sand (%) | 19 | 70 | 41.93 | 9.12 | 21.75 | 0.36 | 0.07 | 0.005 |
| Silt (%) | 16 | 58 | 35.76 | 5.91 | 16.52 | 0.12 | 0.52 | 0.007 |
| Clay (%) | 10 | 37 | 22.29 | 6.14 | 27.54 | -0.13 | -0.77 | 0.014 |
| Gravel (%) | 7 | 24 | 12.8 | 4.6 | 35.93 | 0.85 | 1.25 | 0.003 |
| pH | 7.73 | 8.37 | 8.02 | 0.19 | 2.36 | 0.12 | -0.67 | 0.015 |
| EC (ds/m) | 0.8 | 5.5 | 2.02 | 1.25 | 56.81 | 2.36 | 10.52 | 0.023 |
| Bulk Density (g/cm$^3$) | 1.43 | 1.79 | 1.6 | 0.08 | 5 | -0.04 | -1.06 | 0.025 |
| Organic Matter (%) | 0.12 | 0.53 | 0.42 | 0.33 | 78.54 | 1.96 | 4.60 | 0.005 |
| Carbonates (% ) | 9.5 | 37.3 | 17.48 | 3.22 | 18.42 | 0.77 | 3.82 | 0.031 |

### *Precipitation and temperature data*

Daily precipitation and temperature datasets were acquire from the water resource management bureau of Iran. The daily precipitation data from 67 climatological stations in the Simineh-Zarrineh catchment were utilized to analyze the precipitation variability from 2015 to 2017. The total monthly and daily precipitation, in addition to the daily maximum, minimum, and mean temperature for each month, were employed as meteorological variables in all the . The location of the stations in each sub catchment is shown in Figure 1a.

### *Monitoring soil moisture*

Monitoring the SMAP soil moisture dataset focused on the monthly and seasonal variations in all the subcatchments and was done for a three-year period. The determination the coefficients between SMAP dataset and precipitation were computed using the monthly and seasonal mean, respectively. Furthermore, standard deviation (SD) of the mean annual soil moisture was considered; according to these values for each point, spatial variability of SD was shown with SD map. The spatial distribution and temporal variability in SMAP data from 2015 to 2017 over the catchment in the seasonal scale were analyzed through the kriging interpolation approach via the spatial analysis tools of ArcGIS 10.4. Determination analysis was utilized to find the association among the annual, seasonal, and monthly precipitations and satellite soil moisture over all the subcatchments of the catchment. A positive r value showed that the means were directly correlated and vice versa. The values near zero implied less correlation. The spatial and temporal variability of precipitation and SM for the study period was also considered to explain the dependency of SM on precipitation.

All SMAP soil moisture datasets at different subcatchments were normalized with the minimum and maximum SM, as predicted from the SMAP data was computed for each subcatchment in the period of 2015 to 2017. The normalized soil moisture ($SM_{i(t)}$) was determined using the following equation:

$$SM_{i(t)} = \frac{m_{vi(t)} - m_{vmini(t)}}{m_{vmaxi(t)} - m_{vmini(t)}} \quad (1)$$

where $m_v$ is the SMAP soil moisture for position i at each time (t), $m_{vmin}$ is the minimum SMAP soil moisture value recorded for all the data, and $m_{vmax}$ is the maximum SMAP soil moisture value recorded for the study period (2015 to 2017).

## Results and Discussion

### *Monthly variations of SM*

Figure 2 illustrates the monthly variations of SMAP soil moisture and precipitation for all the subcatchments. As could be seen, the temporal variation of SM is subject to precipitation variation throughout the months. The relationship between soil moisture and precipitation in catchment scale has been well investigated in previous studies (Su *et al.* 2016; Lei *et al.*, 2020). In the Simineh-Zarrineh catchment, precipitation was mainly in the cold season (from October to April) when soil is proportionately wetter and evapotranspiration rate is low. SM undoubtedly relies not only on precipitation, but also on the surface water balance of precipitation, evapotranspiration, and runoff. In hotter months (from June to September), high temperature can intensify the evapotranspiration rate. As shown in Figure 2a, the amount of monthly precipitation ranged from 45 to 80 mm in the Bokan subcatchment from October 2015 to April 2016. There was much less precipitation in the June 2016 to October 2016, amounting to less than 10 mm per month. This result is consistent with those reported by Su *et al.* (2016) who studied the spatial variability of soil moisture content in Tarim river basin in China. They revealed that the lowest and highest precipitation in all the subcatchments occurred between May and October and November to April respectively.

In Figures 2 (a), (b), and (c) the precipitation in October 2015 increases, but the rise in SM is completely coordinated by the precipitation in this month. It would be a large amount of precipitation during dry season in summer and early fall, much of which disappears due to high evaporation and percolation. Figure 2c shows that in January and February 2017, despite the precipitation event in Takab subcatchment, the soil moisture content tends to zero. It would be because of the presence of snow cover on the ground, which affects the accuracy of the satellite sensor during data acquisition (Wang *et al.*, 2018). The Saeinqaleh subcatchment has a moderate climate (with 334.7 mm precipitation and 11.5 ◦C temperature) and consequently, the rate of evapotranspiration is lower than that in the other subcatchments. Thus, the monthly average of soil moisture is high and when a small portion of precipitation occurred, soil moisture content significantly increased. Figure 2e exhibits that even though precipitation does not occur from June to August, the Miandoab subcatchment has higher monthly average soil moisture than all the other subcatchments. This is attributed to proximity and influences of the hydrological cycle of the Urmia Lake and being located in lowland areas, where receive the upland surface runoff. Moreover, irrigation for agricultural crops using the two rivers (Zarrineroud and Simineroud) increases soil water content in this subcatchment.

### *Seasonal variations of SM*

Table 2 summarizes the statistics of SMAP soil moisture in all the seasons. The average and standard deviation (SD) of SM in the summer was obviously the lowest value, indicating the minimum water content and SM fluctuation. SD would be the best indicator studying SM proximity to the mean annual while focusing on the mean precipitation (Wang *et al.*, 2018). In addition, variation in SM was very low in this season, which could be associated with the higher evapotranspiration rate and the lack of precipitation. Variation of SD in autumn was very high; it belongs to the irregular precipitation events and fluctuation of temperature whereas in summer, SD variation was very low, which would be attributed to the lack of precipitation event and the regular increase and decrease in the temperature in the catchment. Briefly, higher values of SD for soil moisture showed large variations of soil moisture in the study period, which can be related to further variations in meteorological variables (precipitation and temperature).

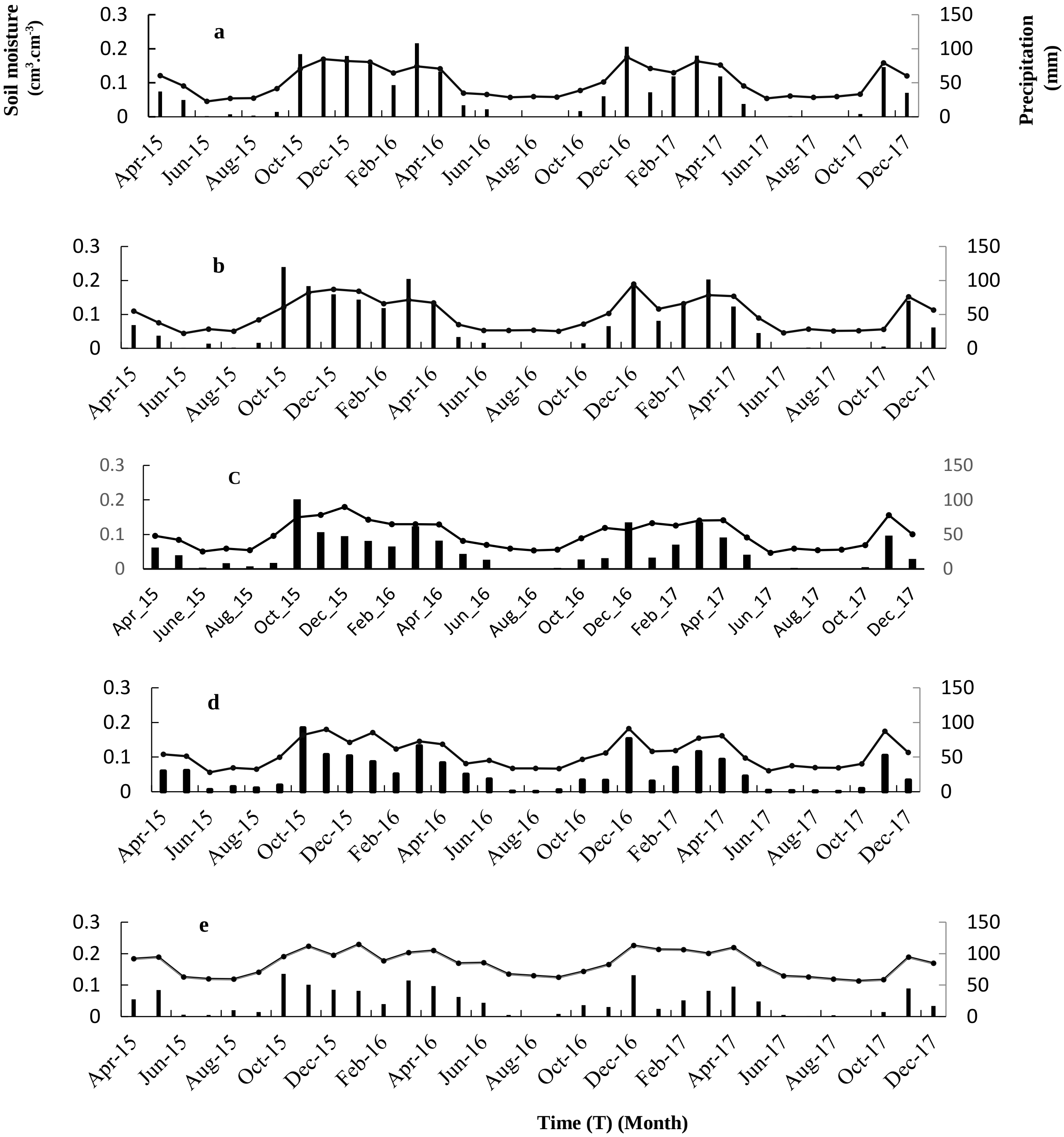


**Figure 2.** Monthly variations of soil moisture and precipitation for all the subcathment of Simineh-Zarrineh catchment: Bokan (a) , Saqqez (b), Takab (c), Saeinqaleh (d), and Miandoab (e) during the study period from 2015 to 2017. SMAP soil moisture and precipitation are shown with black line and bars, respectively

**Table 2.** Summary of the statistics of SMAP soil moisture in the period from 2015 to 2017 over Simineh-Zarrineh catchment

| Season | Year | Min | Max | Mean | Standard Deviation |
|---|---|---|---|---|---|
| Spring | 2015 | 0.04 | 0.24 | 0.1 | 0.05 |
| | 2016 | 0.05 | 0.25 | 0.12 | 0.05 |
| | 2017 | 0.05 | 0.29 | 0.12 | 0.06 |
| Summer | 2015 | 0.04 | 0.18 | 0.08 | 0.03 |
| | 2016 | 0.05 | 0.14 | 0.07 | 0.01 |
| | 2017 | 0.05 | 0.1 | 0.07 | 0.01 |
| Autumn | 2015 | 0.07 | 0.29 | 0.16 | 0.05 |
| | 2016 | 0.05 | 0.28 | 0.11 | 0.05 |
| | 2017 | 0.05 | 0.26 | 0.11 | 0.05 |
| Winter | 2015 | 0.1 | 0.22 | 0.14 | 0.02 |
| | 2016 | 0.12 | 0.16 | 0.15 | 0.01 |
| | 2017 | 0.11 | 0.21 | 0.14 | 0.03 |

The seasonal variations of the SMAP soil moisture and precipitation were monitored in all the subcatchments, which are shown in Figure 3. The minimum soil moisture was observed in summer (from 2015 to 2017). Although in all the graphs, the lowest soil moisture content is in summer, considering that most precipitation occurs in autumn and winter, soil moisture increases in these seasons. According to Figure 3, only in 2015, soil moisture content in winter is approximately equal to that in autumn while in the other years' winter, the highest soil moisture was observed in the subcatchments. Figures 3c and d show the decreasing soil moisture content in autumn to winter 2015; it would be due to high precipitation and low evapotranspiration in autumn (Albergel *et al*., 2013). Summer is a dry season when soil is proportionately drier than that in spring, autumn, and winter so that the lowest amount of soil moisture was seen in summer. This seasonal variation is considerably transparent compared to the other temporal variability in the SMAP data. It would be on account of the fact that the SMAP data are based on a small interval of three days, which may have further uncertainty than the mean SMAP data across a large area. Su *et al.* (2016) found similar results in this regard. They analyzed spatio-temporal variation of soil moisture and its possible influential factors from 1988 to 2013. They revealed that in the period from 1988 to 2013, the soil moisture shows obvious increasing trends in the northwestern and southwestern parts of Tarim River basin, particularly in spring (March-May) and autumn (September-November). In Figures 3 c and d, the reduction in soil moisture content from spring to summer 2015 is unclear due to high summer intrinsic soil moisture content or the precipitation events.

Figure 3e depicts that soil moisture in the Miandoab has a relatively high variability with low precipitation. It appears that soil moisture in this subcatchment is often more than that in the other subcatchments while the precipitation in this subcatchment is lower than that in the the others. Figures 2e and 3e do not show any encounter between soil moisture diagram and precipitation bars; an opposite trend is quite evident in the other charts. Reduction in soil moisture content from winter to spring in this period was not clear, which could be due to specific meteorological and hydrological conditions of this subcatchment. As shown in Figure 3, the decreasing and increasing patterns of soil moisture content in 2016 and 2017 were consistent with precipitation patterns in these years.

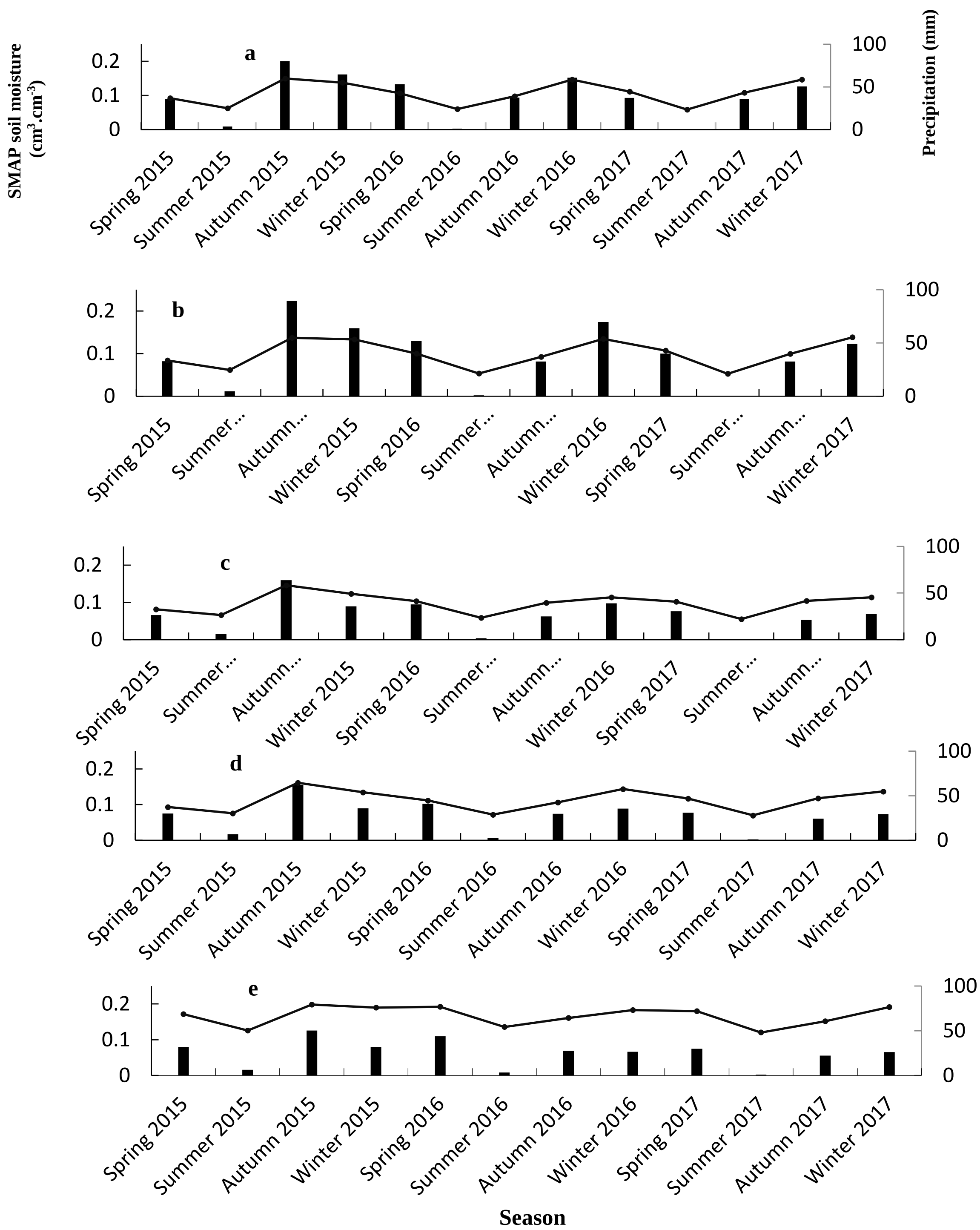


**Figure 3.** Seasonal variation of soil moisture and precipitation for all the subcathments of Simineh-Zarrineh catchment, Bokan (a), Saqqez (b), Takab (c), Saeinqaleh (d), and Miandoab (e) from 2015 to 2017. SMAP soil moisture and precipitation are shown with black lines and bars, respectively

*Spatial distribution of soil moisture*

Spatial distribution of the seasonal SM from 2015 to 2017 is illustrated in Figure 4. Seasonal soil moisture patterns indicated high soil moisture content in the north and particularly northwest areas of Simineh-Zarrineh catchment in all the seasons and decease gradually from west to east. On the contrary, lower SM was observed in the south of the Simineh-Zarrineh catchment and the minimum was in the southeast in all the seasons. The distinctive soil moisture distribution gives an encouraging interpretation for such as land cover configuration; soil water that provides more water supplies for the vegetation growth. As shown in Figure 4, the medium to low SM covered more than a third of Simineh-Zarrineh catchment and these areas were scattered not only in the northern, but also in the southern areas. The areas with a high level of SM covered small parts of this catchment and were situated in the northwest edge and northern section of the catchment. Soil moisture was estimated through the SMAP in spring, summer, and autumn. Quite similar spatial patterns were observed, but in winter, it was different (Figure 4). In spring, all of the snow and frozen soil start to melt when the phenomena of evapotranspiration and percolation are not strong; therefore, the SM average increases. Champagne *et al.* (2016) investigated this issue. They examined two satellite surface soil moisture data sets from the SMOS and Aquarius missions against in situ networks in large agricultural regions of Canada. Their results demonstrated that in early drying events, when all the snow is melted, SM average increases.

The range of SM spatial distribution in spring 2016 was larger than that in other springs. In spring 2015, SM in the northwest and southeast increased and decreased, respectively. However, SM in the south area declined obviously due to the increasing evapotranspiration caused by very high temperature. In autumn 2015, SM increased in the northern and southern parts. With regard to the land surface water balance, SM could be described as the remaining precipitation minus percolation and evapotranspiration (Seneviratne *et al*., 2010). Large scale evapotranspiration is essentially restrained by the accessibility of SM and energy (Seneviratne *et al.*, 2010). The main factors of SM variations are precipitation and energy, which enhanced evapotranspiration. Due to the lack of awareness net radiation at land surface, 2-m air temperature is used like a proxy of accessible energy. Higher temperature raises atmospheric requirement of vapor and leads SM to decrease (Brocca *et al.,* 2012).

Figure 4 demonstrates that the northern part of the catchment located in Miandoab subcatchment had a higher level of SM in all the seasons. This is because of its proximity to Urmia Lake and also more vegetation cover and the fact that most of the area is irrigated agricultural land use (Figure 1a). The southern part of Simineh-Zarrine catchment also located in Saqqez subcatchment had a low level of soil moisture in all the seasons because this sub catchment has a completely irregular topography and most of the area is for pasture land use. However, SM increases annually from summer to spring. Generally, the increased soil moisture in the northwestern area was more obvious than that in the other areas. The spatial distribution of the SM values for 2015 ranged from 0.064 to 0.443, 0.052 to 0.327, 0.121 to 0.402, and 0.109 to 0.446 $cm^3$for spring, summer, autumn, and winter, respectively. In all the seasons of 2015, the southwest and south of Simineh-Zarrine catchment had a minimum soil moisture content, which could be due to hilly land and low vegetation cover.

In all the seasons of the studied period, soil water content decreased from north to south in the Simineh-Zarrine catchment. Nevertheless, from east to west of this catchment, no such constant pattern was observed. It is notable that the decreased and increased SM patterns in this period were completely in line with the precipitation pattern. In Miandoab subcatchment, although precipitation is less, the average soil moisture is high and there is more precipitation. However, the average soil moisture content is less, which could be due to the soil physic-chemical properties and the hydrological conditions.

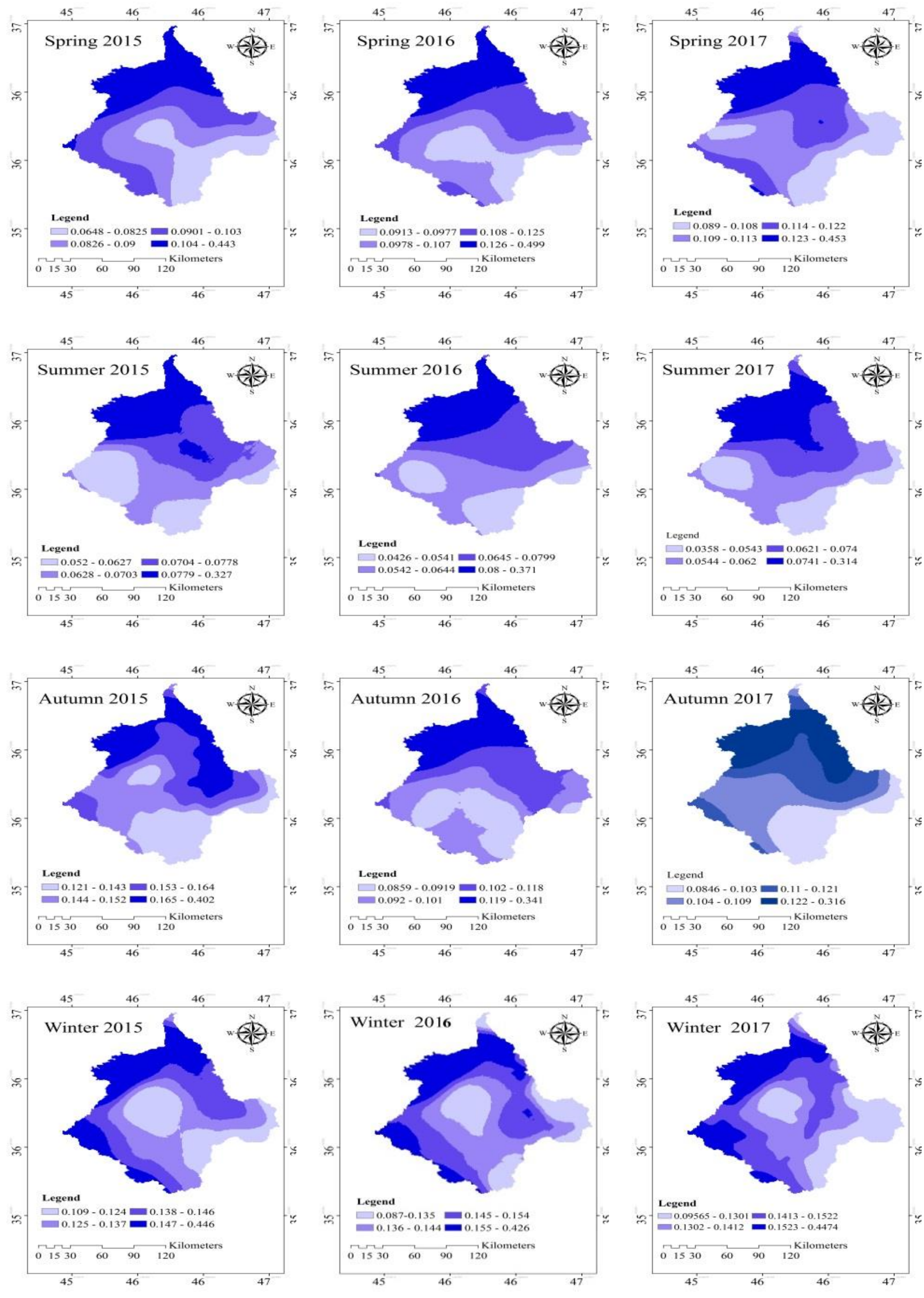


**Figure 4.** Spatial distribution of SMAP soil moisture in Simineh-Zarrineh catchment in seasonal scale from 2015 to 2017

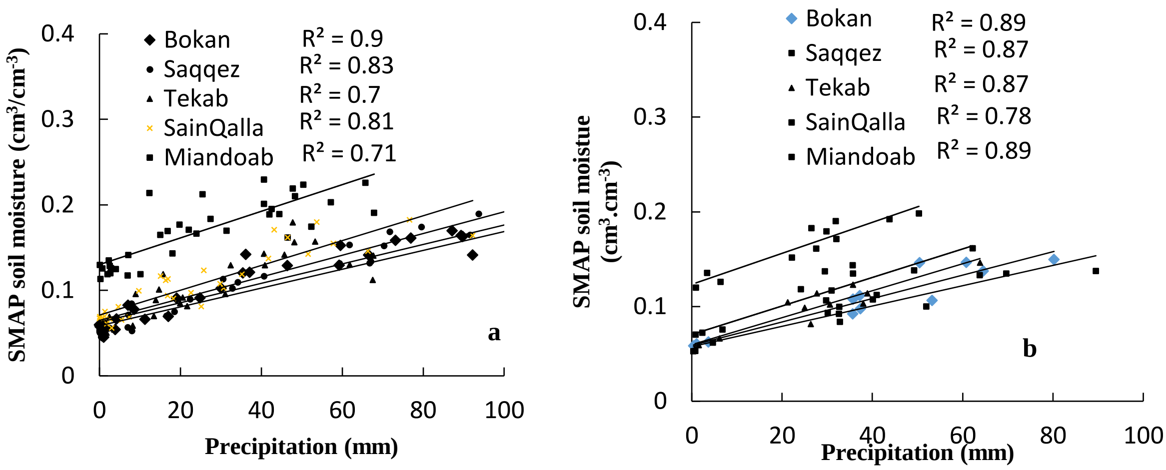


**Figure 5.** Correlation between SMAP soil moisture and precipitation in monthly (a) and seasonal (b) scale for all the subcatchments of Simineh-Zarrineh catchment

Figure 5 represents the determination of the coefficient for linear fitted line between monthly and seasonal average SMAP soil moisture and precipitation for all the subcatchments. In the monthly scale, soil moisture showed a relation with an $R^2$ of 0. 9, 0.83, 0.7, 0.81, and 0.71 for Bokan, Saqqez, Takab, Saeinqaleh, and Miandoab subcatchments, respectively. In the seasonal scale, soil moisture indicated an $R^2$ of 0.89, 0.87, 0.87, 0.78, and 0.89 for Bokan, Saqqez, Takab, Saeinqaleh, and Miandoab subcatchments, respectively. Moreover, the SMAP soil moisture and precipitation indicated a relation with $R^2$ values of 0.86 and 0.81 in spring and autumn, respectively, perfectly showing the correlation of the two datasets in different seasons.

Stronger relationships between monthly or seasonal soil moisture and precipitation in certain areas, such as Bokan subcatchment, demonstrated higher dependency of soil water content to precipitation in longer rainfall periods (spring). In this period, the rate of evapotranspiration is relatively lower and agricultural practices, especially irrigation of crops, is lower (Su *et al*., 2016). In summer, the determination of the coefficient among SM and precipitation data for Saeinqaleh was just 0.76; nevertheless, it indicated a good concurrence yet. When there is no precipitation, the soil is still wet. The reason behind this could be the moisture retained in the soil, which was not affected by precipitation; for instance, in Miandoab, this soil moisture value was more than that in the other subcatchments. This subcatchment is located in low land and the source of soil moisture is the surface currents of the upper subcatchments as well as their irrigation and suitable vegetation.

*Spatiotemporal variability of meteorological variables*

The variations of SM, precipitation, and temperature were investigated to obtain further understanding about the dynamics of SM in the catchment (Figures 6 and 7). The SMAP data and climatological datasets from 2015 to 2017 were utilized in this study. The spatial structure of SM was anticipated to associate with the structure of precipitation and temperature. Figure 6 shows the three-year mean spatial structure of the monthly mean SMAP soil moisture and the monthly mean temperature (◦C) from April 2015 to December 2017. Furthermore, as shown in Figures 2 and 3, soil moisture variations are subject to precipitation variations; on the other hand, soil moisture variability is in good agreement with precipitation variability.

Figure 6 indicates the monthly variability of SM versus temperature. These data recommended that the monthly SM variability in the Simineh-Zarrine catchment are mainly balanced by precipitation. Temperature also has a poor effect on the regulating SM variability. Su *et al*. (2016) obtained similar results studying Tarim river basin of China. The maximum precipitation belonged to October 2015 while the temperature was not low. This is mainly the result of the increased water supply from precipitation rather than intensified evaporated water result by temperature. As shown in Figure 6, in some months, such as February and December 2016 with lower temperature, the increased soil moisture content is not regular. The main reason of this issue might be related to melting of snow and the changes in soil physical properties (structure and porosity) caused by the changes in soil temperature during a day and night in this study area (Reichle *et al*., 2015). However, a comprehensive investigation is needed to confirm this assumption.

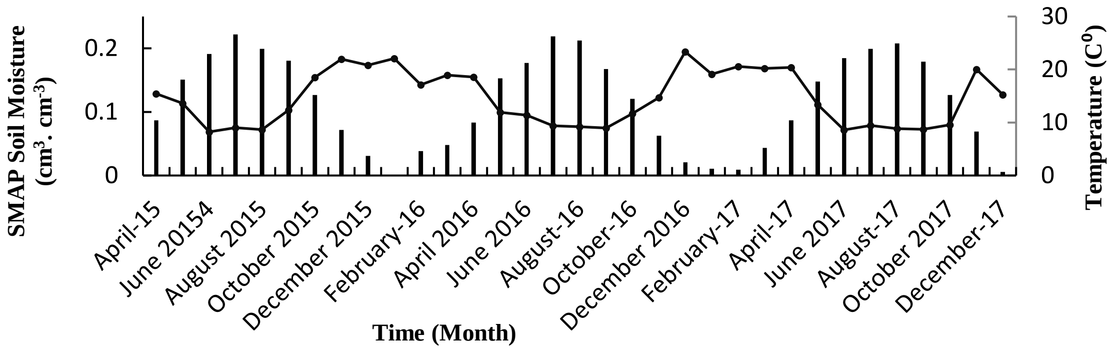


**Figure 6**. Spatial structure of the monthly mean SMAP soil moisture (cm$^3$. cm$^{-3}$) and the monthly mean precipitation (mm) (a); Figure 6: Spatial structure of the monthly mean SMAP soil moisture (cm$^3$. cm$^{-3}$) and the monthly mean temperature (◦C) in the Simineh-Zarrineh catchment from April 2015 to December 2017. SMAP soil moisture and temperature are shown with black lines and bars, respectively

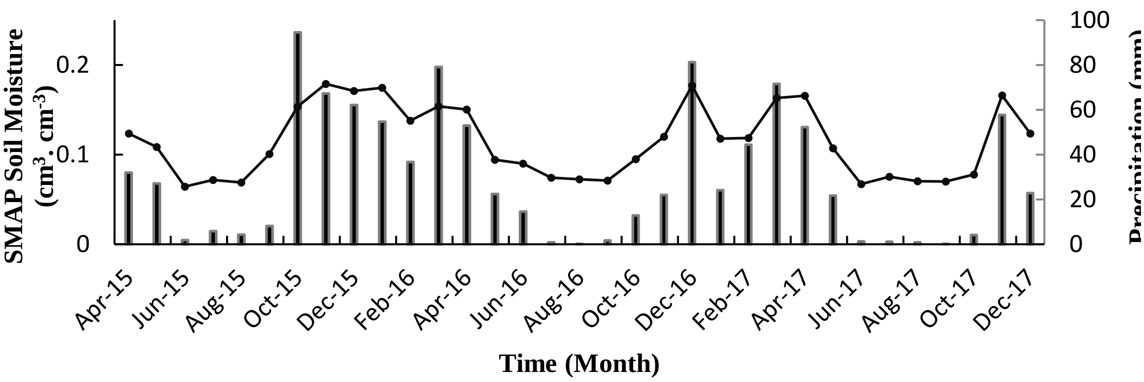


**Figure 7.** Spatial structure of the monthly mean SMAP soil moisture (cm$^3$. cm$^{-3}$) and the monthly mean precipitation (mm) in the Simineh-Zarrineh catchment from April 2015 to December 2017. SMAP soil moisture and precipitation are shown ith black lines and bars, respectively

*Standard deviation of soil moisture*

Figure 8 exhibits the spatial distribution of standard deviation for seasonal soil moisture in Simineh-Zarrineh catchment from April 2015 to December 2017. Obviously, northwestern and eastern parts of the study area had higher values of the standard deviation, indicating a large spatial variability of soil moisture in these areas related to high variation of topography, vegetation, and soil properties. According to Figure 8, soil moisture content of these parts was relatively high in spring. The results indicated that the standard deviation variability was higher in the northwestern parts of Simineh-Zarrineh catchment and most other areas had a lower standard deviation in summer. The values of standard deviation in spring, summer, autumn, and winter ranged from 0.026 to 0.069, 0.011 to 0.063, 0.044 to 0.108, and zero to 0.053, respectively. Based on our findings, a high value of standard deviation was observed in autumn. The reason could be irregular precipitation events, especially in the central parts of the catchment and in the northeastern parts because of proximity to Urmia Lake. On the contrary, the relatively low value of standard deviation was seen in winter with low vegetation covers, which may be on account of snow cover and low evapotranspiration in this season (Su *et al*., 2015). Additionally, the accuracy of SMAP satellite sensor in the presence of snow covers is reduced in this season (Entekhabi *et al*., 2010).

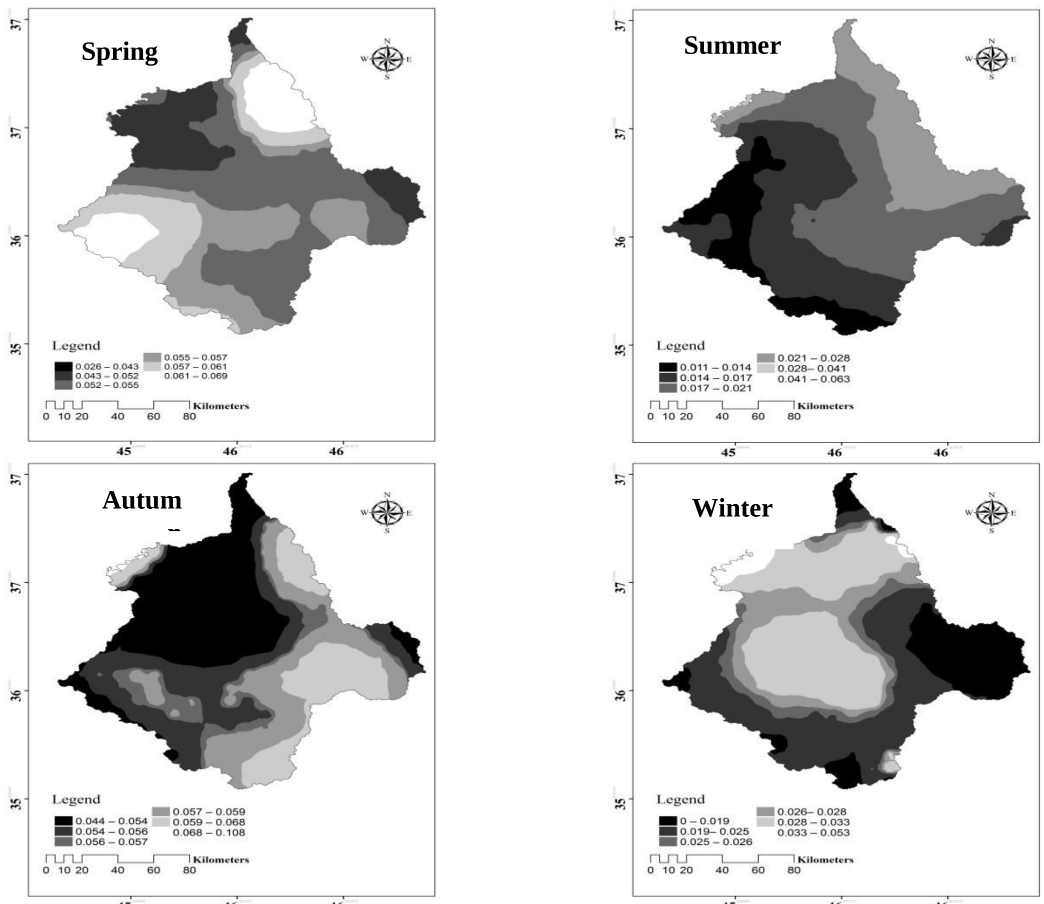


**Figure 8.** Spatial distribution of the standard deviation of SMAP soil moisture in the mean seasonal scale from 2015 to 2017 over Simineh-Zarrineh catchment

## Conclusion

Remotely sensed long-term soil moisture is believed to be an efficient tool for monitoring plant growth condition from space. In this research, the SMAP soil moisture was monitored and analyzed from April 2015 to December 2017 in Simineh-Zarrineh catchment. In all the subcatchments, the results revealed that the SMAP soil moisture was in good agreement with precipitation related to the seasonal and monthly variability; this is indicative of dry soil in summer and proportionately wet soil in autumn, winter, and spring. The SM data of SMAP were in accordance with the variation of precipitation concerning their seasonal variability; this remotely sensed data from SMAP satellite perfectly retrieved the events of dry and wet condition and the monthly variations existing in the precipitation. There is also quite well concurrence of monthly changes among the SM and precipitation, particularly in spring and autumn. The comparison of SM to the temperature data indicated the reliability of this remotely sensed data in the Simineh-Zarrineh catchment. Despite the restricted SMAP soil moisture accessible in this research, the outcomes adequately recommended the ability of the SMAP soil moisture to indicate dynamics of water cycle in large scales. The results also implied that precipitation and temperature have a critical function in regulating the spatio-temporal variability of SM in the Simineh-Zarrineh catchment. In addition, there are several other factors that can affect SM, such as wind speed, aspect, and slope. However, some other factors may have an ancillary role. This was not considered in this research because of data accessibility. In the period from 2015 to 2017, the SMAP data indicated a significant increase in the northwestern and northern parts of the Simineh-Zarrineh catchment, particularly in spring and autumn. Spatial distribution of soil moisture standard deviation in Simineh-zarrineh catchment showed that the northwestern and eastern parts of the study area had obviously high value of the standard deviation. There are highly concentrated irrigated agricultural lands in the center of the Simineh-Zarrineh catchment, which will be irrigated particularly in summer. This may also shed light on the variability in the SM data; this is nevertheless on the far side of this research scope and needs to be further studied in future investigations.

## References

Albergel C, Dorigo W, Balsamo G, Mu˜noz-Sabater J, de Rosnay P, Isaksen L,Wagner W. 2013. Monitoring multi-decadal satellite earth observation of soil moisture products through land surface re analyses. Remote Sensing Environment, 138; 77–89.

Al-Yaari A, Wigneron JP, Ducharne A, Kerr Y, de Rosnay P, de Jeu R, Mialon A. 2014a. Global-scale evaluation of two satellite-based passive microwave soil moisture datasets (SMOS and AMSR-E) with respect to land data assimilation system estimates. Remote Sensing Environment, 149; 181–195.

Babaeian E, Homaee M, Montzka C, Vereecken H, Norouzi AA, van Genuchten MT. 2016. Soil moisture prediction of bare soil profiles using diffuse spectral reflectance information and vadose zone flow modeling. Remote Sensing Environment, 187; 218–229.

Brocca L, Camici S, Melone F, Moramarco T, Martínez-Fernández J, Didon-Lescot JF, Morbidelli R. 2014b. Improving the representation of soil moisture by using a semi analytical infiltration model. Hydroly Processes, 28; 2103–2115.

Brocca L, Moramarco T, Melone F, Wagner W, Hasenauer S, Hahn S. 2012. Assimilation of surface- and root-zone ASCAT soil moisture products intorainfall–runoff modeling. Geoscience Remote Sensing, 50; 2542–2555.

Brocca L, Moramarco T, Melone F, Wagner W, Hasenauer S, Hahn S. 2012. Assimilation of surface and root zone ASCAT soil moisture products into rainfall-runoff modelling. IEEE Transactions on Geoscience and Remote Sensing, 50; 2542–2555.

Champagne C, Rowlandson T, Berg A, Burns T. 2016. Satellite surface soil moisture from SMOS and Aquarius: Assessment for applications in agricultural landscapes. International Journal of Applied Earth Observation and Geoinformation. 45; 143–154.

Chen F, Crow W D, Starks PJ, Moriasi DN. 2011. Improving hydrologic predictions of catchment model via assimilation of surface soil moisture. Advances in Water Resources, 34; 526–535.

Das NN, Entekhabi D, Njoku EG, Johnston J, Shi JC, Colliander A. 2014. Tests of the SMAP combined radar and radiometer brightness temperature disaggregation algorithm using airborne field campaign observations. IEEE Transactions on Geoscience and Remote Sensing. 52; 2018–2028.

Das NN, Mohanty BP, Njoku EG. 2008. Characterization of backscatter by surface features in L-band active microwave remote sensing of soil moisture. IGARSS 2008– 2008 IEEE International Geoscience and Remote Sensing Symposium. vol. 2. IEEE, pp. II–817.

Das NN, Entekhabi D, Njoku EG. 2011. An algorithm for merging SMAP radiometer and radar data for high-resolution soil-moisture retrieval. IEEE Transactions on Geoscience and Remote Sensing 49; 1504–1512.

Entekhabi D, Njoku EG, O'Neill P, Kellogg K, Crow W, Edelstein W, Entin J, Goodman S, Jackson T, Johnson J, Kimball J, Peipmeier J, Koster R, McDonald K, Moghaddam M, Moran S, Reichle R, Shi J, Spencer M, Thurman S. 2010. The soil moisture active and passive (SMAP) mission. IEEE Transactions on Geoscience and Remote Sensing 98; 704–716.

Hassan-Esfahani L, Torres-Rua A, Jensen A, McKee M. 2015. Assessment of surface soil moisture using high-resolution multi-spectral imagery and artificial neural networks. Remote Sensing. 7; 2627–2646.

Iran Ministry of Energy, Deputy of water and Wastewater, Macro Planning Bureau 2014. The National Water Master Plan Study in the Aras, Sefidrood, between Sefidrood and Haraz, Atrac and Urmia Basins, Volume 20: Industrial Water Demand and Consumption and Produced Wastewater in Urmia Basin Projection, 2040 Horizion , Report number: 2385070-5120-24878.

Koster RD, Suarez MJ. 2001. Soil moisture memory in climate models. Journal of Hydrometeorology, 2; 558–570.

Koster RD, Dirmeyer PA, Guo Z, Bonan G, Chan E, Cox P. 2004. Regions of strong coupling between soil moisture and precipitation. Science, 305; 1138–1140.

Legates DR, Mahmood R, Levia DF, DeLiberty TL, Quiring SM, Houser C, Nelson E. 2011. Soil moisture: a central and unifying theme in physical geography. Progress in Physical Geography. 35; 65-86.

Lei F, Crow WT, Kustas WP, Dong J, Yang Y, Knipper KR, Anderson MC, Gao F, Notarnicola C, Greifeneder F, McKee LM. 2020. Data assimilation of high-resolution thermal and radar remote sensing retrievals for soil moisture monitoring in a drip-irrigated vineyard. Remote Sensing of Environment, 239; 111622.

Leroux DJ, Kerr YH, Al Bitar A, Bindlish R, Jackson TJ, Berthelot B, Portet G. 2014. Comparison between SMOS, VUA, ASCAT, and ECMWF soil moisture products over four watersheds in US. IEEE Transaction on Geoscience and Remote Sensing 52; 1562–1571.

Liu YY, Dorigo WA, Parinussa RM, De Jeu RAM, Wagner W, McCabe MF, Van Dijk AIJM. 2012. Trend-preserving blending of passive and active microwave soil moisture retrievals. Remote Sensing. Environment. 123; 280–297.

McGinn SM, Shepherd A. 2003. Impact of climate change scenarios on the agro climate of the Canadian prairies. Canadian Journal of Soil Science, 83; 623–630.

Miralles D, van den Berg M, Teuling AJ, De Jeu RAM. 2012. Soil moisture-temperature coupling: A multiscale observational analysis. Geophysical Research Letters, 39 (No. L21707, 2012).

Mladenova IE, Jackson TJ, Njoku E, Bindlish R, Chan S, Cosh MH, Holmes TRH, De Jeu RAM, Jones L, Kimball J, Paloscia S. 2014. Remote monitoring of soil moisture using passive microwave-based techniques—theoretical basis and over view of selected algorithms for AMSR-E. Remote Sensing Environment. 144; 197–213.

Njoku EG, Entekhabi D. 1996. Passive microwave remote sensing of soil moisture. Journal of Hydrology. 184; 101–129.

Owe M, De Jeu R, van de Griend A. 2000. Estimating long term surface soil moisture from satellite microwave observations in Illinois. IAHS-AISH Publication, USA, pp. 394–399.

Powell LR, Berg AA, Johnson DL, Warland JS. 2007. Relationships of pest grasshopper populations in Alberta, Canada to soil moisture and climate variables. Agricultural and Forest Meteorology, 144; 73–84.

Pratt DA, Ellyett CD. 1979. The thermal inertia approach to mapping of soil moisture and geology. Remote Sensing Environment. 8; 151–168.

Pruski FF, Nearing MA. 2002. Climate-induced changes in erosion during the21st century for eight US Art. no. 1298. Water Resources Research, 38; 1298.

Reichle RH, De Lannoy GJ, Liu Q, Colliander A, Conaty A, Jackson T, Kimball J, Koster RD. 2015. Soil Moisture Active Passive (SMAP) Project Assessment Report for The Beta-Release L4_SM Data Product; NASA Technical Report Series on Global Modeling and Data Assimilation, NASA: Houston, 55p.

Robinson DA, Campbell CS, Hopmans JW, Hornbuckle BK, Jones SB, Knight R, Ogden F, Selker J, Wendroth O. 2008. Soil moisture measurement for ecological and hydrological watershed-scale observatories: a review. Vadose Zone Journal. 7; 358–389. http://dx.doi.org/10.2136/vzj2007.0143.

Sang YF, Wang Z, Liu C. 2014. Comparison of the MK test and EMD method for trend identification in hydrological time series. Journal of Hydrology. 510; 293–298.

Su B, Wang A, Wang G, Wang Y, Jiang T. 2016. Spatiotemporal variation of soil moisture in the Tarim River basin, China. International Journal of Applied Earth Observation and Geoinformation. 48; 122–130.

Tan X, Gan TY, Shao D. 2017. Effects of persistence and large-scale climate anomalies on trends and change points in extreme precipitation of Canada. Journal of Hydrology. 550; 453–465.

Taylor CM, De Jeu RAM, Guichard F, Harris PP, Dorigo WA. 2012. Afternoon rain more likely over drier soils. Nature, 489; 282–286.

Tian J, Philpot WD. 2015. Relationship between surface soil water content, evaporation rate, and water absorption band depths in SWIR reflectance spectra. Remote Sensing Environment. 169; 280–289.

Vereecken H, Huisman JA, Pachepsky Y, Montzka C, van der Kruk J, Bogena H, Weihermüller L, Herbst M, Martinez G, Vanderborght J. 2014. On the spatiotemporal dynamics of soil moisture at the field scale. Journal of Hydrology. 516; 76–96.

Verstraeten WW, Veroustraete F, van der Sande CJ, Grootaers I, Feyen J. 2006. Soil moisture retrieval using thermal inertia, determined with visible and thermal space borne data, validated for European forests. Remote Sensing Environment. 101; 299–314.

Wang C, Fu BJ, Zhang L, Xu ZH. 2019. Soil moisture plant interactions: an eco-hydrological review. Journal of Soils Sediments 19; 1-9.

Wang X, Wanga B, Xu X, Liu T, Duan Y, Zhao Y. 2018. Spatial and temporal variations in surface soil moisture and vegetation cover in the Loess Plateau from 2000 to 2015. Journal of Ecological indicators. 95; 320–330.

Whiting ML, Li L, Ustin SL. 2004. Predicting water content using Gaussian model on soil spectra. Remote Sensing Environment. 89; 535–552.

Zeng W, Xu C, Huang J, Wu J, Tuller M. 2016. Predicting near-surface soil moisture content of saline soils from NIR reflectance spectra with a Modified Gaussian model. Soil Science Society of America Journal. http://dx.doi.org/10.2136/sssaj2016.06.0188.

Zhang Q, Li J, Singh VP. 2013. Copula-based spatio-temporal patterns of precipitation extremes in China. International Journal of Climatology. 33; 1140–1152.